Membrane Boundary Extraction Using a Circular Shortest Path Technique

Changming Sun*, Pascal Vallotton*, Dadong Wang*, Jamie Lopez†, Yvonne Ng† and David James†

*CSIRO Mathematical and Information Sciences, Locked Bag 17, North Ryde, NSW 1670, Australia
†Garvan Institute of Medical Research, 384 Victoria Street, Darlinghurst, Sydney NSW 2010, Australia

Abstract. Membrane proteins represent over 50% of known drug targets. Accordingly, several widely used assays in the High Content Analysis area rely on quantitative measures of the translocation of proteins between intracellular organelles and the cell surface. In order to increase the sensitivity of these assays, one needs to measure the signal specifically along the membrane, requiring a precise segmentation of this compartment. Doing this manually is a very time-consuming practice, limited to an academic setting. Manual tracing of the membrane compartment also confronts us with issues of objectivity and reproducibility. In this paper, we present an approach based on a circular shortest path technique that enables us to segment the membrane compartment accurately and rapidly. This feature is illustrated using cells expressing epitope-tagged membrane proteins.

Keywords: Membrane, Membrane assay, High content analysis, Membrane segmentation, Membrane boundary extraction, Circular shortest path.
PACS: 87.15.Kg, 07.05.Pj, 42.30.Sy

INTRODUCTION

The outer lipid bilayer of a cell mediates the exchange of polypeptides, lipids and other molecules and serves as an interface for inter-cell communication. Regulation of these exchanges through modulation of the concentration, activities, and spatial distribution of proteins and lipids within this cell compartment is therefore critical to normal cell function. A majority of drugs available today exert their effect by targeting membrane proteins, mainly by antagonizing the signalling action of soluble hormone-like ligands.

The spatial distribution of membrane proteins within the bilayer plane influences their function. Clusters of high-concentrated membrane proteins underly important cellular processes, including exocytosis, endocytosis, mitosis, and cell migration. Membrane proteins may even be found in a crystalline state within the membrane. Also, upon fixation and staining, the membrane undergoes massive damages that compromise the continuity and uniformity of the membrane compartment. As a result, tracing the membrane of immunostained cells in confocal images is far from trivial.

Young and Gray used semi-automatic boundary detection techniques for identification of cells in differential interference contrast (DIC) microscope images [1]. Wu et al introduced an iterative thresholding algorithm for the segmentation of cells from noisy cell images [2]. Ortiz de Solorzano et al carried out nuclei and cell segmentation by manually identifying seeds and expanding the boundaries of the seeds until they reach

CP952, *Computational Models for Life Sciences—CMLS '07, 2007 International Symposium*
edited by T. D. Pham and X. Zhou

the limits of the nuclei or cells [3]. This is similar to the snakes or active contour type of algorithms [4, 5]. Liang et al used a dynamic programming procedure for boundary detection in ultrasonic artery images [6]. Other approaches related to membrane boundary extraction include those in [7, 8, 9].

In this paper, we propose an approach for membrane boundary extraction using a circular shortest path technique. The use of the circular shortest path technique in the neighbourhood of a cell centre ensures that all the information along an extended region is taken into account. We also provided a mechanism for the use of control points if necessary during the process of boundary extraction.

The paper is organised as follows. We first describe our algorithm for membrane boundary extraction. We then outline the steps of our algorithm. We demonstrate the capabilities of our membrane boundary extraction algorithm on a range of real images in the experimental results section, and then conclude.

MEMBRANE BOUNDARY EXTRACTION

In this section we describe our algorithm for membrane boundary extraction using a circular shortest path technique which ensures that the boundary obtained is closed and has the maximal integrated image intensity along its path.

Approximate Cell Location

We begin by obtaining an approximate position of the centre of the cell. This can be achieved by an interactive step or through an automated process. With the interactive approach, a user can click a point close to the centre of the cell in an image. In an automated approach, the approximate centre of the cell may be obtained by the automated segmentation of the nucleus channel if available. The approximate centre can actually be anywhere within a certain distance of the cell centre. This approximate position of the cell centre will be used next for transforming the input image into polar coordinates to obtain the membrane boundary.

Image Transformation

The neighbourhood around the approximate cell centre is transformed into polar coordinates. Depending on the position of the cell centre in the original image, portions of the transformed image may contain no values. In the transformed image, the top row corresponds to the centre point. The bottom row corresponds to the perimeter of the circular region. The left and the right sides of the transformed image are neighbouring columns. That is, they are from neighbouring radial segments from the approximate cell centre of the input image.

The size of the transformed image depends on the angular resolution and the radius that we specify in the polar coordinate. Figure 1 shows an example of the transformed image in a cell region of the input image. Figure 1(a) is the input image with the small

plus sign indicating the approximate position for the cell centre; and Figure 1(b) is the local region around the cell in polar coordinates.

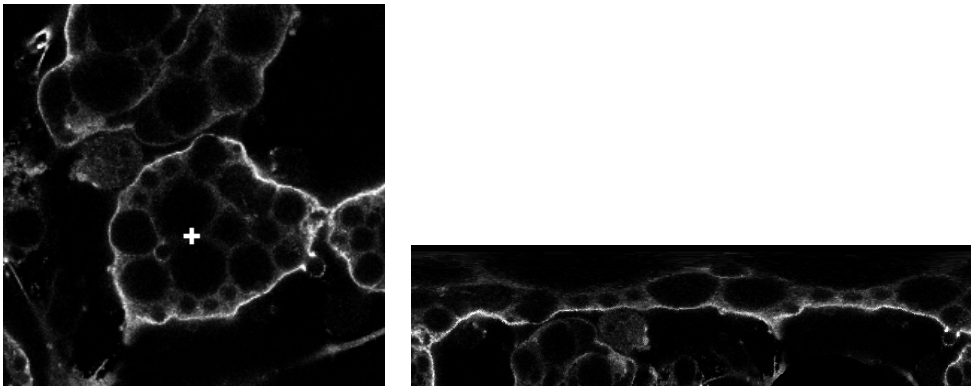

(a) (b)

FIGURE 1. Polar transformed image for a local region of an input image. (a) input image with a cross indicating the approximate centre of cell; (b) polar transformed image.

Boundary Extraction

We obtain a circular shortest path (CSP) from this transformed image for extracting the membrane boundary.

Sun and Pallottino developed several algorithms for circular shortest path extraction on regular grids or images [10]. These algorithms are the multiple search algorithm (MSA), image patching algorithm (IPA), multiple backtracking algorithm (MBTA), a combination algorithm of IPA and MBTA, and an approximate algorithm. We will use the IPA algorithm here for membrane boundary extraction because it is conceptually easy to understand and is very fast. The basic idea behind the IPA algorithm is to carry out image patching, a step which ensures path closure, and use a dynamic programming algorithm to find a path in the patched image.

The patching for the IPA algorithm is carried out in the horizontal direction on the left and the right sides of the transformed image. The values of the patched regions come from the transformed image itself. A shortest path is obtained from this patched image, and a CSP may be extracted from the patched image. For detailed description of the IPA algorithm please see [10].

The steps of the IPA algorithm for CSP extraction in the transformed image are:

1. Patch the transformed image on the left and the right sides with portions of the transformed image itself to obtain a patched image.
2. Perform ordinary shortest path extraction using dynamic programming on the patched image.
3. Extract the shortest path which lies inside the original transformed image.

The pseudo code for obtaining the shortest path in the patched image using dynamic programming is given below.

```
Procedure Shortest Path via Dynamic Programming():
#initialising nodes in the first column:
foreach j ∈ C_1 do
    d_1j := c_1j;
    p_1j := nil;
#obtaining accumulated cost (loop over columns):
for h := 2 to v do
    foreach j ∈ C_h do
        d_hj := c_hj + min_{i∈{|i−j|≤1}}{d_{h−1,i}};
        p_hj := argmin_{i∈{|i−j|≤1}}{d_{h−1,i}};
#picking up the minimum value in the last column and backtracking
```

In this pseudo code, d_{hj} is the accumulated cost for the jth point for the hth column; p_{hj} holds the backtracking information for d_{hj}; v is the number of columns; C_h is the set of pixels in column h; i is the pixel location on the previous column; j is the pixel location on the current, hth, column; and c_{hj} is the connection cost from i to j, and takes the intensity value at position (h, j) in the patched image. The process of obtaining the accumulated cost involves the collection of the current best cost at a point and its backtracking information.

Use of Control Points

Due to noise and the presence of other cells nearby, the extracted membrane boundary may not be optimal. For example, in Figure 3(a), part of the boundary may have shifted to the boundary of other cells due to the fact that the strength of the boundary of the other cell is much stronger than the cell that we are interested in. In this case, we can add one or more control points close to the membrane boundary to enforce the extracted boundary to be close to these control points by assigning special (e.g. large negative) values for some columns of the transformed image except for the pixels that are close to the control points.

MEMBRANE BOUNDARY EXTRACTION PROCEDURE

We outline here the main steps of our algorithm for obtaining membrane boundary from images using the circular shortest path technique. The summary steps of our membrane boundary detection algorithm are the following:

1. Locate the approximate centre of the cell. This can be interactive or automated;
2. Add extra control points close to the membrane if necessary;
3. Transform the input image from Cartesian to polar coordinate system;
4. Apply circular shortest path extraction algorithm to the transformed image;

5. Convert the path obtained to the original image space; and
6. Measure the characteristics of the membrane boundary.

EXPERIMENTAL RESULTS

In this section we present results obtained from images of adipocytes expressing epitope-tagged membrane proteins using our membrane boundary extraction algorithm.

Figure 2 shows an example image of a cell and its membrane boundary, as given in green, obtained using our algorithm. Figure 3 shows the use of control points to regulate the shape of the circular shortest path. Figure 3(a) is the result without the use of control points. The membrane boundary obtained close to the bottom right corner has shifted to a different cell that has a brighter boundary. Figure 3(b) shows two control points in red to be used to help obtain the correct boundary. Figure 3(c) shows the membrane boundary obtained using the two control points. This boundary is very close to the true membrane boundary.

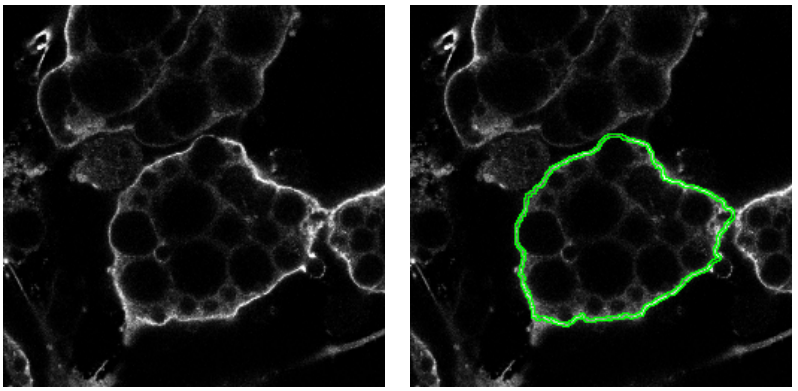

(a) (b)

FIGURE 2. Membrane boundary extraction. (a) input image; (b) membrane boundary extracted and overlaid to the input image.

We have also tested the effect of changing the centre of the cell on the extraction of membrane boundary. It turns out that the position of the cell centre can be quite flexible within the cell. As long as the approximate centre is not too close to the membrane boundary and there is no boundary folding for a particular viewing direction from the centre, our algorithm is most likely able to find the correct boundary.

The running time of our algorithm was tested on an Intel Pentium 4 with a 2.66 GHz CPU under the Linux operating system; and our images were 8 bit/pixel. For a 512x512 pixel image, analysis takes about 1 seconds. For colour images, only the intensity information or a single channel was used.

The measurements along the membrane boundary that are of interest include average intensity, maximum intensity, standard deviation of intensity, integrated intensity, and length of boundary.

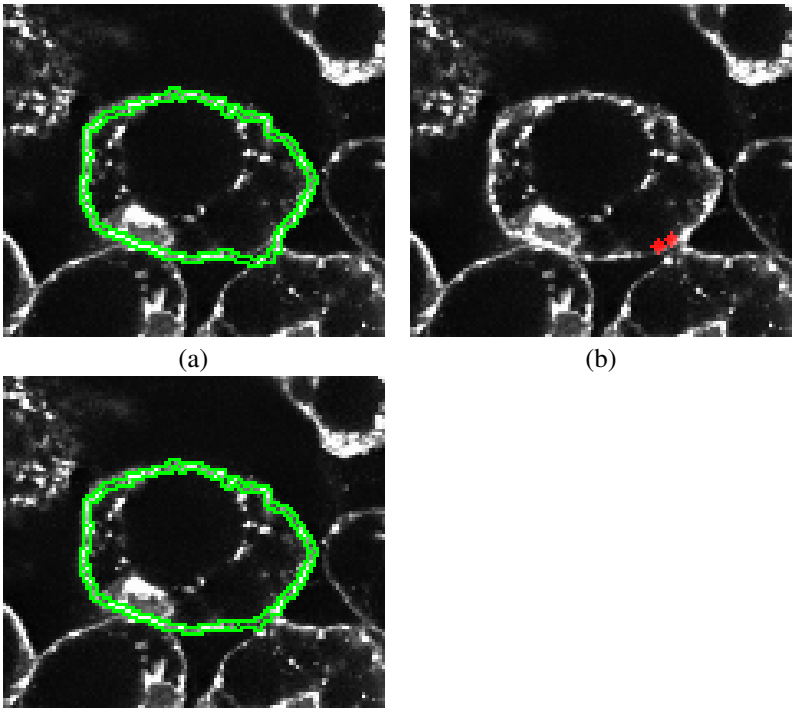

FIGURE 3. Membrane boundary extraction with control points. (a) results without the use of control points; (b) two control points shown in red; (c) results with the use of the two control points.

The use of circular shortest path technique for membrane boundary extraction ensures that the boundary obtained for a cell is a closed contour. The global optimisation property of the shortest path technique via the use of dynamic programming gives the global minima along the membrane boundary unless multiple paths have ties. Because it is a global optimisation approach, small gaps in a local region can be filled and hence generate a continuous boundary. In contrast, techniques using snakes may sometimes stop at local mimima.

The current algorithm ensures that a path obtained in the transformed image is connected. In the future, we plan to introduce a smoothness term to increase the path regularity. Other constraints such as the minimum and/or maximum radius of the cell can be used to further control the boundary.

CONCLUSIONS

We have introduced a new capability for measuring fluorescence signals precisely within the plasma membrane compartment. In our method, the membrane is not defined as the

outer limit of an approximately identified cytoplasm, but rather, it corresponds to an optimal trace with highest integrated intensity. We hope to demonstrate in future experiments that cell based assays developed using our method will display sharper response curves than alternative assays. We are planning to make available the functionalities illustrated in this paper in HCA-Vision, our cell analysis software.

ACKNOWLEDGMENTS

We thank Dr Rongxin Li of CSIRO and conference reviewers for their comments on an early draft of this paper.

REFERENCES

1. D. Young, and A. J. Gray, "Semi-automatic boundary detection for identification of cells in DIC microscope images," in *Sixth International Conference on Image Processing and Its Applications*, Dublin, Ireland, 1997, vol. 1, pp. 346–350.
2. H.-S. Wu, J. Barba, and J. Gil, *Journal of Microscopy* **197**, 296–304 (2000).
3. C. Ortiz De Solorzano, R. Malladi, S. A. Lelièvre, and S. J. Lockett, *Journal of Microscopy* **201**, 404–415 (2001).
4. M. Kass, A. Witkin, and D. Terzopoulos, *International Journal of Computer Vision* **1**, 321–331 (1988).
5. D. J. Williams, and M. Shah, *CVGIP: Image Understanding* **55**, 14–26 (1992).
6. Q. Liang, I. Wendelhag, J. Wikstrand, and T. Gustavsson, *IEEE Transactions on Medical Imaging* **19**, 127–142 (2000).
7. S. Raman, C. A. Maxwell, M. H. Barcellos-Hoff, and B. Parvin, *Journal of Microscopy* **225**, 22–30 (2007).
8. H. Chang, K. L. Andarawewa, J. Han, M. H. Barcellos-Hoff, and B. Parvin, "Perceptual Grouping of Membrane Signals in Cell-based Assays," in *4th IEEE International Symposium on Biomedical Imaging: From Nano to Macro*, 2007, pp. 532–535.
9. N. L. Prigozhina, L. Zhong, E. A. Hunter, I. Mikić, S. Callaway, D. R. Roop, M. A. Mancini, D. A. Zacharias, J. H. Price, and P. M. McDonough, *ASSAY and Drug Development Technologies* **5**, 29–48 (2007).
10. C. Sun, and S. Pallottino, *Pattern Recognition* **36**, 711–721 (2003).